HHS Public Access

Author manuscript

J Immunol. Author manuscript; available in PMC 2024 June 15.

Published in final edited form as:

J Immunol. 2023 June 15; 210(12): 1950–1961. doi:10.4049/jimmunol.2200337.

CD4 Effector TCR Avidity for Peptide on APC Determines the Level of Memory Generated

Michael C. Jones[1], **Catherine Castonguay**[1], **Padma P. Nanaware**[1], **Grant C. Weaver**[1], **Brian Stadinski**[1], **Olivia A. Kugler-Umana**[1], **Eric S. Huseby**[1], **Lawrence J. Stern**[1], **Karl Kai McKinstry**[2], **Tara M. Strutt**[2], **Priyadharshini Devarajan**[1,*], **Susan L. Swain**[1,*]

[1.] Department of Pathology, University of Massachusetts Chan Medical School, Worcester, MA 01605, USA

[2.] Division of Immunity and Pathogenesis, Burnett School of Biomedical Sciences, College of Medicine, University of Central Florida, Orlando, FL. 32827,USA

Abstract

Initial TCR affinity for peptide antigen is known to impact generation of memory, however its contributions later, when effectors must again recognize antigen at 5–8 days post-infection to become memory, is unclear. We examined whether the effector TCR affinity for peptide at this “effector checkpoint” dictates the extent of memory and degree of protection against rechallenge. We made an influenza A virus (IAV) nucleoprotein (NP)-specific TCR transgenic mouse strain, FluNP, and generated NP-peptide variants which are presented by MHC-II to bind to the FluNP TCR over a broad range of avidity. To evaluate the impact of avidity *in vivo*, we primed naïve donor FluNP in IAV-infected host mice, purified donor effectors at the checkpoint and co-transferred them with the range of peptides pulsed on activated APC, into second uninfected hosts. Higher avidity peptides yielded higher numbers of FluNP memory cells in spleen and most dramatically in lung and dLN, and induced better protection against lethal influenza infection. Avidity determined memory cell number, not cytokine profile, and already impacted donor cell number within several days of transfer. We previously found that autocrine IL-2 production at the checkpoint prevents default effector apoptosis and supports memory formation. Here, we find peptide avidity determines the level of IL-2 produced by these effectors and that IL-2Rα expression by the APC enhances memory formation, suggesting that transpresentation of IL-2 by APC further amplifies IL-2 availability. Secondary memory generation was also avidity-dependent. We propose this regulatory pathway selects CD4 effectors of highest affinity to progress to memory.

Keywords

Avidity; Affinity; CD4; T cell; Effector; Memory; IL-2; Transpresentation; Contraction; Survival; Proliferation; Nucleoprotein; Influenza; Immunodominant; Vaccine; FluNP; MHC-II; TCR; T cell receptor

[*]**Corresponding author:** Susan L. Swain, Department of Pathology, University of Massachusetts Chan Medical School, Worcester, MA 01605, USA, Phone: 518-524-1925 (cell) susan.swain@umassmed.edu, Priyadharshini Devarajan, Department of Pathology, University of Massachusetts Chan Medical School, Worcester, MA 01605, USA, Phone: 508-856-4395 (office), priyadharshini.devarajan@umassmed.edu.

Introduction

T cells recognize conserved viral epitopes and hence T cell memory provides broad, heterologous immunity crucial to protection against rapidly mutating viruses including influenza. Resting CD4 T cells respond to infection by generating amtigen(Ag)-specific effectors that protect against infection, via multipe synergizing mechanisms (1), including help to CD8 and B cells, production of IFNγ and perforin-mediated cytotoxicity. After viral clearance, a cohort of CD4 effectors becomes memory cells which can protect against future infections. However, the signals and mechanisms required for the transition of CD4 effectors to memory are only partially defined.

Several studies indicate that longer duration of Ag stimulation during priming results in increased naïve CD4 T cell response, leading to greater proliferation and function of effector cells (2–4). Both the amount of peptide Ag loaded onto MHC-II receptors on an antigen presenting cell (APC), which determines the density of peptide-MHC (pMHC-II) complexes on the APC, and the affinity of the pMHC-II interaction with TCR during priming, determine the extent of T cell response (5). While strong pMHC-II interactions with TCR favor Th1 over Th2 development (6–8), their role in T_{FH} versus Th1 differentiation is less clear, with conflicting reports (9–12). There are also conflicting reports that either strong or weak initial pMHC-TCR interactions better support memory formation and recall responses (11,13–20). Thus, whether the extent of CD4 effector cell transition to memory is dependent on their affinity for Ag is unclear.

Mice infected with influenza present a wide diversity of Ag epitopes to T cells, with high viral titers and Ag presentation,soon after infection that remain high until infection is cleared (21, 22). Infection produces very strong CD4 T cell memory, suggesting that persistent high levels of Ag, may explain the high levels of memory generated Here, we specifically analyze the impact of TCR avidity for peptide on APC at the effector phase, when both viral levels and CD4 effectors have peaked, and when effectors that fail to recognize Ag undergo apoptosis (23, 24). We ask if high vs. low affinity Ag drives generation of more CD4 memory cells and if they provide superior protection. Previously, we showed that to become memory cells, CD4 effectors generated *in situ* by IAV infection, needed to recognize Ag during the effector phase checkpoint, spanning from 5–8 days post infection (dpi), (23, 24). During this cognate interaction, the effectors must produce autocrine IL-2, which prevents their apoptosis, enabling their transition to memory (23–25). Morevoer, we also showed that the addition of short-lived, Ag-pulsed APC at this checkpoint boosted memory formation (23) but that viral infection, apart from its role in cognate Ag presentation, was not required between 5–8 dpi to promote memory (23).

To study the impact of peptide avidity at this crucial juncture, we developed a TCR Tg mouse (FluNP) specific for $NP_{311–325}$, an immunodominant, highly conserved, IAV nucleoprotein (NP) epitope in B6 mice (22). We made a truncation and single amino acid substitutions to generate a library of NP_{311} peptides with a spectrum of functional avidities for the FluNP TCR. We used an adoptive transfer model to generate *in vivo* effectors from naïve CD4 by IAV infection in a first (1^{st}) host, isolated 6 dpi donor effectors and then

co-transferred them to a second (2^{nd}) host (23). Here we used activated APC, pulsed with peptides from a panel spanning high to low avidity for the FluNP TCR, as the only source of Ag.

We find that APC with higher avidity peptides at 6d of the CD4 effector response, promote a far larger CD4 memory population in the spleen, lung and dLN, and that this leads to better protection upon influenza rechallenge. The peptide affinity and dose used to pulse APC determines the level of IL-2 produced by the 6d effectors, and the levels of IL-2 correlate with the prevention of default effector apoptosis, survival and development of memory (24). CD25, the high affinity IL-2 receptor (IL-2Rα), is not expressed on 6d CD4 effectors, but is highly upregulated on APC in IAV-infected 4–8 dpi mice. Holding the peptide Ag constant, APC expressing CD25 generated higher numbers of CD4 T cell memory than CD25 deficient APC. We propose that IL-2Rα expression on APC acts in concert with IL-2Rβ/γ on the effector CD4 cells, to enhance availableIL-2 and signaling. We suggest that at the effector phase, the level of IL-2 production, determined by peptide affinity, and efficacy of the response to autocrine IL-2 enhanced by IL-2 transpresentation, are the dominant pathways that regulate the size of the memory CD4 population. We discuss the implications of this requirement for high peptide affinity at the effector stage for vaccine design that promotes protective CD4 memory with a focus on kinetics, Ag breadth and adjuvants that activate APC.

Materials and Methods

Mice

We use 8–12 wk old C57BL/6 (B6) mice as hosts in all experiments. Naive CD4 T cells are isolated from B6.FluNP strains, including B6.FluNP.Thy1.1$^{+/-}$ and B6.FluNP.Nr4a1^{EGFP}.Thy1.1$^{+/-}$. The B6.Nr4a1 ^{EGFP} developed by Kris Hogquist and Steve Jameson (26) were from Jackson Laboratories. BMDC were derived from B6 or B6.129S4-*Il2ra*^{tm1Dw}/J (CD25KO) mice obtained from The Jackson Laboratory and bred at UMMS breading facility. Mice used in experiments were 8–12 wk of age. The Institutional Animal Care and Use Committee of UMMS approved all animal procedures.

B6.FluNP TCR Tg mice were generated in collaboration with Eric Huseby's Laboratory at UMMS. Briefly, B6 mice were infected with a sub-lethal dose of PR8 (0.3 LD_{50}) and at 21 dpi, 2×10^7 spleen and lung draining lymph node (dLN) cells were isolated and stimulated *in vitro* with irradiated spleen cells loaded with 100 ug/ml $NP_{311–325}$ peptide. After 5 days, responding T cells were fused with BW5147 to generate T cell hybridomas (27). T cell hybridomas with reactivity to $NP_{311–325}$ peptide, presented by lung APC from IAV-infected mice (A/PR8/34)-infected mice, were expanded. TCR Vβ-chains were identified by staining with a set of Vβ-specific Abs (BD Biosciences), and the TCRα-chains were identified by PCR analysis using a panel of TCR Vα primers that collectively amplify all TCR Vα gene families. We choose a hybridoma with Vα4.2 and Vβ2.1. A TCR Tg plasmid was made using cloned rearranged cDNAs for 22.B6 TCR Vα4.2 and Vβ2.1. Vα4.2 (Arden), included the V region TRAV6–5, CDR3(CALRSSGSWQLIF) and J region(IMTG): TRAJ22. Vβ2, included TCRV (Arden):TRAV1, CDR3 (CTCSAEVGGDTQYF) and J region (IMTG): TRAJ2–5. Cloned products were fused with full length TCR Cα and Cβ sequences (28). All

the TCR genes were sequenced, and error-free full-length cDNAs were subcloned into the human CD2 promoter transgene cassette for T cell–specific expression (29). B6.FluNP were established by injecting C57BL/6 oocytes with the TCR-Tg plasmid.

Virus Stocks and Infections

Mice were anesthetized with either isoflurane (Piramal Healthcare) or ketamine/xylazine (at a dose of 25/2.5 mg/kg by i.p. injection) before i.n. infection with 50 μl of influenza virus diluted in PBS corresponding to a 0.2 to 0.3 (sub-lethal) medial lethal dose (LD_{50}) for response, $2LD_{50}$ for weight loss, and $4LD_{50}$ for survival. Influenza virus A/Puerto Rico/8/34 (PR8, H1N1), originally from St. Jude Children's Hospital, was from our stocks grown and maintained at the Trudeau Institute. The virus was also characterized by its ability to infect eggs, and we found $2LD_{50}$ corresponds about 10,000 EID_{50}. Our standard dose sub-lethal $0.3LD_{50}$, corresponding to 25 PFU.

NP Peptide Generation

We modified the $NP_{311–325}$ peptide to produce peptides of shorter lengths by deletions of amino acids (aa) on both ends to determine the best length. We used single alanine substitutions to determine the peptide-I-A^b binding frame (P1=**Y**), then selective aa side-chain modifications, at known peptide-TCR contact positions to generate peptides likely to have lower affinities. Peptide-I-A^b IC_{50} was determined with surface plasmon resonance (SPR) using a BIAcore 3000. SPR analysis was performed using a BIAcore 3000 instrument (Cytiva). Briefly, biotinylated, peptide exchanged MHCs were immobilized on a streptavidin chip. For the TCR, the FluNP TCR sequence was cloned into the pCDH lentiviral expression vector with a P2A site separating the alpha and beta chains. This construct was used to generate stable lines in 293S GnTI cells. TCR was then purified from supernatant with a nickel-NTA column and subsequent size exclusion. Recombinant FluNP TCR was then passed over at increasing concentrations. A5 was used as a negative control and the signal from this flow cell was subtracted from those of experimental flow cells. The resulting data points were plotted and fitted to hyperbolas to derive K_Ds.

BMDC Generation and Peptide/APC Preparation.

APC were generated as in (23, 30) BM was harvested from B6 or CD25KO mice, washed with RPMI 1640, 1% FBS and cells plated at10^7 cells/mL in RPMI with 10% FBS and 10 ng/mL GM-CSF. After 7d, $CD11c^+$ BMDC were isolated via MACS and activated with polyinosinic-polycytidylic acid (PolyI:C) at 10 μg/mL overnight in culture or use as APC. APC were pulsed with a standard concentration of 100 μM or dilutions thereof, of each of a chosen panel of NP peptides. For *in vivo* experiments pulsing was at 37°C for 1hr with shaking, APC were washed 3x, resuspended in PBS, and 1×10^6 cells injected i.v. per mouse.

Sequential Transfer Model

We closely followed the model we developed previously (23). Spleens and peripheral lymph nodes (LN) were collected from B6.FluNP.Thy1.$1^{+/-}$ mice. Naïve CD4 cells were isolated via negative selection with CD4 MACS (Miltenyi Biotec and washed 3x, resuspended in

PBS. 0.5–1 × 10^6 naïve CD4 cells were transferred via i.v. injection into B6 1st hosts. 1st hosts were infected with a sub-lethal dose of PR8 the same day. Donor CD4 effectors were re-isolated from the 1st hosts at 6 dpi. Single cell suspensions were prepared from pooled spleen and dLN and donor FluNP cells were isolated via Thy1.1 positive selection by MACS (Miltenyi Biotec). Cells were resuspended in PBS and 1.5 × 10^6 donor FluNP cells per mouse injected into 2nd B6 hosts i.v., along with Ag/APC (peptide-pulsed). To maintain effector phenotype all steps were conducted at room temperature, except for one 15 min incubation at 4°C. This minimal protocol, without sorting, ensures that effector cells are only out of mice for a maximum of 2.5 hours. IL-2 complexes (IL-2:anti-IL-2 Ab) treatment was administered daily, at 5–7 dpi, as previously described (24).

In Vitro Culture of Naïve and 6 dpi effector FluNP CD4 T cells.

To assess functional avidity of peptides, we compared their ability to induce responses of FluNP naïve CD4 T cells, isolated as described above (sequential transfer model). Following isolation of naïve or 6d FluNP effectors and generation of Ag/APC, cells in complete RPMI 1640 media were plated at a CD4 T:APC ratio of 5:1. Following 2d in culture, plates were centrifuged, supernatant was removed for cytokine protein analysis via ELISA and cell pellets were stained for FACS analysis.

ELISA

Supernatants were collected from *in vitro* culture. Plates (Nunc) were coated overnight with capture antibody (ELISAmax Biolegend). The following day plates were blocked following the manufacturer's protocol and supernatants were added neat, or diluted 1:10, 1:100, 1:1000 and left at 4°C overnight. The following day plates were washed, and detection protocol was followed per manufacturer's protocol.

Flow Cytometry and Cytokine Staining

Cells were harvested, passed through a 70 μm cell strainer and stained in FACS buffer (0.5% Bovine Serum Albumin, 0.01% sodium azide (Sigma Aldrich) in PBS. Cells were blocked with anti-FcR (2.4G2) and stained with amine reactive viability dyes (Invitrogen) to exclude dead cells. Surface proteins were stained with fluorochrome conjugated antibodies at 4°C. Antibodies used included anti: CD4 (GK1.5 and RM), CD44 (IM7), CD90.1 (OX-7 and HIS51), CD11c, CD25, CD62L, CD69, CD80, CD86, CD122, CD132, CD185 (CXCR5, SPRCL5), NKG2A/C/E, MHCII (I-A^b). For CD127 staining, anti-CD127-Biotin was included in the surface stain mixture, cells were washed 3x, and a secondary fluorochrome conjugated SA was used in the second step. For cytokine staining, total splenocytes were stimulated with 10 μM of $NP_{311–325}$ for 6 hr at 37°C. Brefeldin A (10 μg/mL) was added after 1 hr of stimulation. Following surface staining, cells were fixed in 2% paraformaldehyde for 20 min and permeabilized with 0.1% saponin buffer (1% FBS, 0.1% NaN_3 and 0.1% saponin in PBS (Sigma Aldrich) for 15 min. Subsequent staining for cytokines using the following antibodies: anti-IFNγ (XMG1.2), anti-TNFα (MP6-XT22), anti-IL-2, anti-IL-17. For transcription factor staining cells were first surface stained then fixed and permeabilized using FoxP3 fix/perm kit (eBioscience) overnight per manufacturer's protocol and stained with the following antibodies: anti-BCL-6 (K112–91), anti-FoxP3, anti-T-bet at 4°C for 1 hour. Antibodies obtained from BD Bioscience,

Biolegend and eBiosceince. Stained cells were acquired on a BD LSRII flow cytometer and analyzed using FlowJo analysis software.

Statistical Analysis

Groups of at 3–5 mice were used in all experiments, and exact conditions repeated to obtain sufficient statistical power. All experiments shown were repeated 2–3 or more times. For statistical analysis an unpaired, two-tailed independent t test was used. All analysis was performed using GraphPad's Prism.

Results

Characterization of FluNP TCR Transgenic CD4 T cell Response

We generated a B6 TCR transgenic (Tg) mouse specific for an immunodominant NP core protein epitope, $NP_{311–325}$, from the internal nucleoprotein (NP) of influenza PR8/34 (H1N1) presented by I-A^b (MHC-II). This epitope is conserved among all dominant outbreak strains of IAV in people (22) and in the IAV strains we use. The mouse was created by selecting T cell hybridomas specific for $NP_{311–325}$ from IAV-infected mice (27–29). We call the mouse FluNP.

We generated B6.FluNP.Thy1.1/Thy1.2 mice so we could readily detect donor FluNP cells by flow cytometry after transfer to second hosts by their Thy1.1 expression. To evaluate whether IAV induces a comparable response of the donor FluNP cells and polyclonal host CD4 T cells, we transferred naïve FluNP CD4 T cells into hosts and infected with a sub-lethal dose of PR8/34, a mouse-adapted influenza A virus (IAV). We compared the kinetics of donor FluNP TCR Tg and endogenous host ($CD4^+$ $CD44^{hi}$) T cell responses 4, 6, 8, 12, 21 and 63 days post infection (dpi) in the lung (Fig. 1A), draining mediastinal lymph node (dLN) and spleen (Supp. Fig. 1A). IAV infection induced a similar pattern of expansion and contraction of donor FluNP and host CD4 T cells in the lung (Fig. 1A), and spleen and dLN (Supp. Fig. 1A). We assessed the subsets of CD4 effectors generated from both donor FluNP and host naïve CD4 T cells at 8 dpi, by their cytokine production and phenotypic markers. We enumerated Th1 (T-bet, IFNγ, TNFα, IL-2), triple cytokine producers (IFNγ, TNFα, IL-2), Th17 (IL-17), and T_{REG} (FoxP3). We also used NKG2A/C/E expression to detect cytotoxic CD4 (ThCTL), which we found only in the lung (31), and CXCR5 and Bcl-6 co-expression markers to detect T_{FH} in the spleen (32) (Fig. 1B, Supp. Fig. 1B–I). Both donor and host responses in the lung were dominated by Th1 phenotype cells (33–35), with high expression of T-bet, IFNγ and TNFα (Fig. 1B, left, Supp. Fig. 1B, E), and little expression of IL-17 or FoxP3 (Fig. 1B, left, Supp. Fig. 1D) markers of Th17 and Treg. ThCTL in lungs were found in both at similar proportions (Fig 1B, left, Supp. Fig. 1C). In the spleen, donor and host subset patterns were also similar (Fig 1B, right, Supp. Fig. 1F–I). Thus, the overall effector responses of donor monoclonal FluNP and host polyclonal CD4 to IAV were comparable.

We examined memory populations at 21 dpi, assessing phenotypically distinct memory subsets: central memory T_{CM} ($CD127^+$ $CD44^+$ $CD62L^+$), effector memory T_{EM} ($CD127^+$ $CD44^+$ $CD62L^-$) and resident memory T_{RM} ($CD44^+$ $CD69^+$). The overall patterns in donor

and host memory were again similar, (Fig. 1C, Supp. Fig. 1J–M) and both donor and host memory cells expressed high levels of the canonical CD4 memory marker CD127 (~75%), in all tissues (Supp. Fig 1L). Together these comparisons of donor FluNP and host polyclonal response support the conclusion that FluNP CD4 T cells respond equivalently to host polyclonal ones and that this model is suitable for investigate the impact of peptide avidity on memory generation.

Generation of a Panel of NP Peptides With a Broad Range of Avidity for FluNP TCR

To study the role of peptide avidity at the checkpoint in promoting memory generation, we first generated a series of NP peptides with single amino acid (aa) substitutions that have a broad range of abilities to stimulate the naïve FluNP response when pulsed on B6-derived activated APC. We sought substitutions that altered TCR interaction while maintaining tight peptide-MHC interaction. First, we identified the I-A^b binding frame by scanning partially overlapping 11-residue peptides that cover the full $NP_{311–325}$ peptide for I-A^b binding, using a fluorescent peptide competition binding assay and purified recombinant I-A^b carrying a cleavable linker peptide (36). I-A^b binding was substantially reduced for $NP_{313–323}$ and lost completely for $NP_{314–324}$, (Fig. 1D) suggesting that Y_{313} occupied the key P1 position in the I-A^b binding site (37, 38). We confirmed this using alanine-scanning mutagenesis, revealing Y_{313} as the only position where I-A^b binding was substantially affected (Fig. 1D). To identify peptides that modulate TCR interaction, we introduced other substitutions in addition to alanine at the predicted TCR contact positions P2 (SerGln), P5 (ArgLys), and P7 (GluGln). Some of these substitutions caused moderate reductions in peptide-MHC binding, up to 3.4 for Q2 (Fig. 1D). To evaluate the effect of these substitutions on FluNP TCR interaction independent of peptide-MHC effects, we measured pMHC-TCR binding using a surface plasmon resonance (BIAcore) assay with streptavidin-immobilized biotinylated I-A^b-peptide complexes and recombinant soluble FluNP TCR (Fig. 1E). FluNP TCR bound to I-A^b carrying the parent $NP_{311–325}$ peptide or truncated $NP_{311–322}$ (NPT) with high affinity (K_D ~ 3uM) (Fig. 1E). The other substitutions at predicted TCR contact position caused reductions in pMHC-TCR affinity ranging from ~20-fold (for A7) to >150-fold (for Q7). The A5 substitution abrogated detectable binding.

We ranked the substituted NP peptides by their ability to stimulate a FluNP response (functional avidity). We loaded bone marrow derived dendritic cells (BMDC) activated with poly I:C, with peptides over a broad dose range and evaluated how well they stimulated naïve FluNP cells *in vitro*. After 2d, we assessed induction of CD69 (Fig. 1F), CD25 (IL-2Rα) (Fig. 1G) and Nurr77 (Fig. 1H). By all three assays of naïve CD4 T cell activation, FluNP CD4 T cells responded in a dose and affinity dependent manner. Thus, we could confidently rank the relative avidity of the peptide-MHC-II complex on APC for the FluNP TCR on the CD4 T cells. We classify the NPT and $NP_{311–325}$ as high avidity, A7 and K5 as medium (mid) avidity, Q2 and Q7 as low avidity, and use A5 and unpulsed BMDC as negative controls. In each assay, the high peptides (NP_{311} and NPT) induce peak responses at doses 100-fold lower than the middle peptides (A7, K5), and the low peptides (Q2, Q7) require 10 times the dose as the two middle peptides (Fig. 1F–H).

From here on, we use a high dose of 10^{-4} M to pulse APC, to minimize the contribution of peptide density and maximize the contribution of pMHC-TCR affinity. At this concentration, all 6 peptides (NPT, $NP_{311–325}$, A7, K5, Q2, Q7) stimulate a measurable FluNP naïve CD4 T cell response.

Peptide Avidity at the Effector Phase Determines the Number of Memory Cells.

We evaluated the impact of peptide avidity on *in vivo* memory generation using a sequential adoptive transfer model, developed previously (23). Naïve FluNP were transferred to 1st hosts, infected with IAV to generate 6d effectors *in vivo*. These were purified by flow cytometry based on their expression of Thy1.1 and were were co-transferred to uninfected 2nd hosts with groups of peptide-pulsed APC as the only source of Ag (23) (Fig. 2C). The APC are short-lived and present Ag for only 48–72h (23), defining the discrete checkpoint for effectors to recognize Ag we have established is necessary for memory generation. To compare the number of FluNP memory cells generated from high avidity peptide/APC to those generated by IAV infection, we transferred 6 dpi FluNP effectors into either 6 dpi PR8 infection-matched hosts, vs uninfected hosts along with high affinity peptide-pulsed NPT/APC (Fig. 2A). At 21 dpi, NPT/APC stimulated FluNP effectors produced as many memory cells in spleen and lung and only slightly fewer in dLN as PR8 infection (Fig. 2B). Thus, a high avidity peptide/APC generates an equivalent number of memory cells from effectors as does IAV infection, both here and in an equivalent model using OT-II Tg CD4 T cells (23).

We investigated if modulating avidity over a broad range would lead to a corresponding influence on donor memory numbers in the 2nd hosts in the same model (Fig. 2C). The impact of peptide avidity was striking, with numbers of recovered memory cell clearly dependent on the rank of the peptides. The greatest differences in memory cell number were seen in the lung, followed by the dLN, and lastly the spleen (Fig. 2D–E, Supp. Fig. 2A). The significance of these changes between groups of peptides is illustrated by the fold change in memory cell number between each peptide-pulsed APC, compared to unpulsed APC: (Fig. 2F, left), to low peptides (2F, right) and to middle peptides (Fig. 2F bottom). In the lung, there were 280-fold more donor FluNP cells in the NPT-pulsed group compared to the unpulsed group, 29 and 36-fold more compared to the low groups, and 6 and 8-fold more donor memory cells compared to the mid groups. A nearly identical pattern was seen in the dLN. In spleen, there were 16-fold more FluNP cells in the NPT group compared to the unpulsed group and 5–8-fold to the mid groups, both highly significant (Fig. 2E–F). These data indicate that the strength of pMHC-TCR interaction at the effector checkpoint determines the size of the memory population, in all both secondary lymphoid organs and in lung, but that the effect is most dramatic in lung and dLN.

We analyzed the donor-deived memory cells for surface phenotype. They uniformly express high CD127, the IL-7Rα, which supports CD4 memory generation in the secondary lymphoid tissues (39), in all stimulated groups in the spleen and dLN (Fig 2 C–E), while in the lung many donor cells do not express CD127 as expected (40). We assessed cytokine production *ex vivo* by the memory cells stimulated with different peptides on APC by intracellular cytokine staining (ICCS) (Supp. Fig. 2F–H). Overall, all memory cells

produced equivalent levels of IL-2, TNFα, and IFNγ. The high affinity peptide resulted in only a slightly higher fraction of IFNγ-capable memory. Overall, these results suggest the even the memory cells that develop at lower avidity are likely to be functional if they encounter sufficient Ag on restimulation.

Peptide Avidity at the Effector Checkpoint Promotes Effector Cell Survival.

To probe the mechanisms by which peptide avidity has such a dramatic impact on memory cell recovery, we asked if affinity impacts FluNP effector cell proliferation, survival, or both (Fig. 3A). To evaluate proliferation, we stained the 6d donor effectors with cell trace violet (CTV) before transfer and examined their division *in vivo* 3d after co-transfer with Ag/APC. As indicated by dilution of CTV, the spleen FluNP cells in each peptide group divided multiple times, while the unpulsed group barely proliferated (Fig. 3B). Thus, proliferation of transferred cells required Ag recognition, but peptide avidity did not impact the pace or numbers of division in any organ (Supp. Fig. 3A–C). These results suggest, the dramatic differences in memory cell numbers (Fig. 2), are not due to a greater rate or number of cell divisions.

We determined survival of FluNP effectors by measuring expression of caspase 3/7 and viability stain at 3d after transfer (Fig. 3C, Supp. Fig 3D–F). In the spleen, we found a much greater fraction of live, caspase 3/7 negative cells in the NPT (high) and A7 (mid) groups compared to the Q2 (low) group (Fig. 3C, Supp. Fig. 3D), indicating there is greater apoptosis in the low avidity group compared to both mid and high groups. Most donor cells recovered in the unpulsed APC group were pro-apoptotic by 3d post-transfer (dpt) (Fig. 3C), consistent with a strict requirement for Ag recognition to prevent effector apoptosis (23). We did not see a clear difference in cell survival with different affinity peptides on APC in dLN or lung, although all peptides led to higher survival than APC with no peptide (Supp. Fig 3E–F). Perhaps the response kinetics are different in each organ, or the spleen is a major source of memory generation after which developing memory cells migrate to the lung and dLN. Therefore, we also evaluated donor cell recovery as a more integrated measure of net survival. We found a clear-cut pattern with recovery corresponding to higher peptide avidity in all sites (Fig. 3D) that was of similar magnitude at 3 dpt (late effector) as it was at 15 dpt (memory) (Fig. 2E). We conclude that the impact of peptide avidity in regulating memory cell recovery is realized within a few days of effector cell Ag encounter, and it is primarily due to the fraction of effectors that survive rather than to their extent of division.

Peptide Avidity at the Effector Checkpoint Induces More Effector IL-2 Production.

Effector phase autocrine IL-2 signaling is required for CD4 T cell memory development and that autocrine IL-2 acts by downregulating pro-apoptotic Bim, which promotes the survival of effector CD4 survival (23, 24). We thought this likely requires IL-2Rα expression on the effectors (24). Therefore, we analyzed the expression of IL-2R subunits CD132 (IL-2Rγ), CD122 (IL-2Rβ) and CD25 (IL-2Rα) on donor FluNP effectors before transfer and 3d after *in vivo* stimulation with the various peptide/APC. Before restimulation, 15% of FluNP effectors express CD132, 40% expresses low levels of CD122 but <10% express CD25 (Fig. 3E). Following stimulation with high affinity peptide/APC *in vivo*, three-quarters of FluNP cells in lung at 3 dpt strongly express CD132 and almost all express CD122 (>90%)

(Fig 3E), regardless of the avidity of peptide used to stimulate them. But again, few FluNP effectors in spleen and lung express CD25 (Supp. Fig. 3G), and only half are $CD25^+$ in the dLN (Fig 3E, Supp. Fig. 3G). In the *in vivo* setting, we found no difference in IL-2R subunit expression on 3 dpt donor cells following high, mid and low TCR signaling in any tissue, and even the unpulsed group 3 dpt effectors expressed a similar pattern (Supp. Fig. 3G). These findingd suggest that avidity does not act by upregulating IL-2R chain expression and leave unresolved the mechanism by which autocrine IL-2 effectively signals the effectors.

We examined the impact of peptide avidity on the level of IL-2 produced by 6d effectors. We restimulated 6d FluNP effectors *ex vivo* with the panel of NP peptide-pulsed APC introduced in Fig. 1, and quantified IL-2-producing cells by ICCS (Fig. 3F) and levels of secreted IL-2 by ELISA (Fig. 3G–H). The fraction of IL-2-positive 6d FluNP effectors corresponded closely with increasing peptide avidity, mirroring the impact on memory. Thus, induction of IL-2 secretion by FluNP effector cells is highly dependent on the avidity of Ag recognition. Since the CD4 T cell response is also dependent on density of peptide Ag/MHC we varied the peptide concentration used to pulse the APC (Fig. 3G, Supp. Fig. 3J). We found that peptide dose also strongly influenced IL-2 production by the 6d effectors. With higher avidity peptides, higher levels of IL-2 were made and they increased with concentration so they were detectable even at very low dose (10^{-7} M), while with while mid and low peptides much higher concentrations were required. We integrated the area under the curve, as a reflection of overall IL-2 that could be (Fig 3H). This confirmed IL-2 production mirrored the rank of peptides determined by measures of affinity and functional avidity (Fig. 1). As peptide avidity determines the level of autocrine IL-2 produced, and since IL-2 availability determines their survival (24), this is likely the key pathway that translates the peptide avidity into the number of memory cells generated following influenza infection. IFNγ and TNFα production were also dependent on peptide avidity and on dose (Supp. Fig 3H–I), indicating the a general avidity dependence for the elicitation of cytokine production at the effector stage.

IL-2 Complex Addition Can Overcome Lower Peptide Avidity for Effector TCR.

In the *in vivo* response to live influenza autocrine, but not paracrine IL-2 produced by co-transferred WT CD4 T cells, supports CD4 effectors to efficiently transition to memory (24). However when high levels of additional IL-2 are provided as a complex (IL-2c) that has extended bioavailablity at 5, 6 and 7 dpi, IL-2-deficient CD4 T cells responding against influenza, can develop into memory cells (**current ref 47**). We reasoned that, if as we suggested above, the impact of peptide avidity acts by enhancing IL-2 production during cognate effector: Ag/APC interation, treating mice in which CD4 effectors responding to low avidity peptides with IL-2c should enhance memory. To test this, we transferred 6 dpi FluNP effectors along with high avidity NPT/APC or with low avidity Q2/APC to 2^{nd} hosts. One group of 2^{nd} hosts that received Q2/APC was also treated with IL-2c for 3d after cell transfer. We assessed donor cell memory generation at 21d (Fig 4A–D). As before, CD4 memory generated in response to low affinity Q2-APC was dramatically lower in all sites versus that generated in mice recieving NPT-APC. Importantly, the addition of IL-2c enhanced memory generation to the low avidity peptide significantly so the level was nearly comparable to the high avidity response.

CD25 Expression on APC During the Effector Phase Promotes Effector Transition to Memory.

When effector cells recognize peptide Ag presented by APC, they make IL-2 within several hours, which traditionally was predicted to bind to the tripartite IL-2R on the same cell, since the IL-2 needs to be autocrine (24). However, we see in Fig 3E, the 6d FluNP effectors do not express CD25. IL-15 shares two-thirds of its receptor (IL-2Rβ/γ) with IL-2 and is known to be transpresented by IL-15Rα on APC to IL-2Rβ/γ on T cells (41–43). Several previous studies found that IL-2 can also be transpresented and speculated that this impacts responses by limiting (45) or augmenting IL-2 availability(46). We asked if IL-2 transpresentation might play a role during the cognate interaction of CD4 effectors with peptide/APC. We first analyzed whether IAV infection generates CD25-expressing APC. In uninfected mice, we found no CD25 expression on MHC-II$^+$ cells but 6d after infection a cohort of dLN CD11c$^+$, MHC-II$^+$ cells clearly express CD25 (Fig. 4E). At 4–8 dpi, the time when autocrine IL-2 signals are needed for CD4 T cell memory (47), substantial populations of CD11c$^+$, MHC-II$^+$ cells express CD25 in the lung, dLN and spleen (Fig 4F).

To analyze whether CD25 expression on APC plays a role in CD4 effector survival to memory, we generated 6d FluNP effectors and co-transferred them with WT or *CD25*$^{-/-}$ activated APC (BMDC) pulsed with high and mid NP peptides (Fig. 4G). Both APC expressed high levels of CD11c, MHC-II, CD80 and CD86, but only WT BMDC expressed CD25 (Supp. Fig. 4A). We found that 6d effectors stimulated *in vitro* with WT vs *CD25*$^{-/-}$ peptide/APC produced equivalent amounts of IL-2 and IFNγ (Supp. Fig 4B–C) indicating that both activate FluNP similarly. However, when we assessed *in vivo* generation of memory in the transfer model with WT or *CD25*$^{-/-}$ APC (Fig. 4G–J), significantly fewer donor memory cells developed in spleen, dLN and lung of 2nd hosts when NPT high and middle avidity peptides were presented by *CD25*$^{-/-}$ BMDC (Fig. 4H–J), with more dramatic differences in dLN and lung and lessor-fold diffences in spleen. The fraction of donor memory cells that produced IL-2, IFNγ and TNFα was equivalent (Supp. Fig 4D–F). This provides clear evidence that transpresentation of IL-2 by APC during cognate interaction serves to amplify the IL-2 signal to the CD4 effectors and this leads to generation of more memory cells

Peptide Avidity at the Effector Checkpoint Determines Protection from Influenza Challenge.

We asked if 2nd hosts of FluNP effectors which receive higher avidity peptide/APC arebetter protected from rechallenge with IAV. We generated memory from FluNP effectors co-transferred with high or low Ag/APC (Fig. 5A). After 21 dpi, we challenged the mice with a sublethal dose of PR8 and analyzed their weight loss (Fig. 5B). The high avidity group recovered weight significantly faster than the low group, and both recovered more rapidly than the unpulsed group (Fig. 5B). When we challenged hosts with a higher, lethal dose of PR8 and analyzed survival, more animals in the two high groups (>80%) survived compared to their two low signaling counterparts (50–60%) and these were better protected than unpulsed APC (20%) (Fig. 5C). Thus, higher avidity peptide at the effector phase promoted a more protective memory FluNP population and the degree of protection increased with the

size of the memory population. This supports the concept that peptide avidity determined functioning memory.

Peptide Avidity During Ag Recognition by Secondary Effectors Determines Their Memory Generation.

Memory CD4 T cells have less stringent requirements than naïve cells for Ag dose and costimulatory interactions (48), and they become more protective secondary effectors during re-infection with influenza (49). Influenza-specific memory T cells accumulate with age in humans due to multiple exposures and their longevity, through both influenza infections and vaccinations (50–52) and thus may dominate responses. We asked whether avidity of TCR for peptide determines the level of memory generated from secondary effectors cells. We generated primary memory cells from 6d FluNP effectors with high peptide/APC in the 2nd host, whose polyclonal CD4 T cells remained otherwise naïve. After 21d, we infected these 2nd hosts and isolated 6d donor secondary effectors. We co-transferred the donor secondary 6d FluNP effectors along with high, mid and low avidity peptide-pulsed APC or unpulsed APC (Fig 6A) into 3rd hosts and enumerated 2° memory FluNP after 21d in the spleen, dLN and lung (Fig. 6B). In each organ, memory generation was dependent on Ag recognition as expected (49z), with the high peptide NPT producing 14.4-fold more memory in spleen, 40-fold more in dLN and 34-fold more in lung compared to APC with no peptide Ag. Thus like naïve cells, CD4 memory cells, need to recognize Ag again as secondary effectors, during the defined kinetic window we call the effector checkpoint, to form optimal secondary memory and the avidity of TCR for peptide Ag, again determines many the amount secondary memory cells that are formed.

Discussion

We examined the impact of peptide avidity for the FluNP TCR, delivered by peptide-pulsed APC at the CD4 effector checkpoint (23, 24), on memory formation. Our earlier studies established that peptide-pulsed poly I:C activated APC added at the effector checkpoint, generated memory equivalent to that primed by infection (23,24), and showed that peptide-pulsed APC used as here, efficiently presented Ag to transferred 6d effectors in the spleen, resulting in a strong systemic response like that ot infection (32). We recovered the greatest number of CD4 memory cells after 6d effecters were stimulated with the highest avidity peptide, with 200-fold more in the lung compared to no peptide, and 20–50-fold more compared to low avidity peptide. Higher avidity drove higher levels of autocrine IL-2 production, which promoted greater effector survival and donor cell recovery in the late effector phase, laying out the mechanisms likely to be responsible.

The importance of autocrine IL-2 in memory formation was emphasized by the fact that optimum levels of memory required that activated APC express IL-2Rα during the cognate interaction with CD4 effectors that express IL-2Rβ/γ but not CD25 the IL-2Rα. Higher avidity also led to increased protection from lethal rechallenge. Secondary CD4 effector cells derived from memory cells, also required Ag recognition to form secondary memory and were also favored by high avidity peptide. To increase CD4 T cell memory, we suggest

vaccine strategies must supply a second round of high avidity Ag and pathogen recognition signals from infection, during the effector stage of CD4 T cell response.

Previous studies varied Ag avidity at the initiation of the immune response and found that higher levels and avidity could led to greater effector and memory cell number (53–56). Extending the period of Ag presentation also promoted enhanced CD4 and CD8 memory formation (2–4, 23, 24, 57, 58). The pathways responsible were not determined and we know of no studies by others that restricted Ag to the effector checkpoint 6–8 dpi, that we showed is strictly required for memory generation (23, 24, 47) and is when the TCR avidity for peptide/APC has striking impact shown here. Our study is the first to analyze the effect of a broad range of affinities during the effector checkpoint on memory formation. Our results indicate that at the effector checkpoint, 6 dpi after initial infection, CD4 effector TCR avidity for peptide/MHC-II on APC during cognate interaction determines the magnitude of memory by regulating the level of effector production of autocrine IL-2. In turn, this determines how many effectors survive over the next few days and progress to memory. Autocrine IL-2 at the effector stage is also required in polyclonal responses (24), so we suggest this is a universal mechanism to select for CD4 memory cells that are of the highest affinity for the pathogen Ag epitopes they recognize.

In our studies, the impact of peptide avidity on memory was consistently more dramatic in lung and dLN, compared to the spleen. One likely explanation for this is that higher avidity peptide also promotes effector migration from the spleen to the lung, so the impact is less apparent in the spleen. We and others have shown that checkpoint Ag recognition and strong Th1 skewing promote greater expression of CXCR3 by effector cells which promotes their trafficking to tissue sites (23, 35, 59, 60). The results are particularly striking here, because in the 2^{nd} host there is no infection or inflammation in the lung to attract effectors. Thus, we suggest peptide avidity at the effector checkpoint also regulates migration to the tissues. A previous study indicated that high affinity of responding CD8 effectors for Ag was associated with prolonged proliferation, delayed contraction and migration (62), suggesting a parallel mechanismmay occur in CD8 memory formation.

We found previously that Ag presentation to effector CD4 T cells at the effector checkpoint induces autocrine IL-2 production, which prevents their default apoptosis and thus supports formation of memory cells (24). IL-2 from co-administed WT TcR Tg cells could not rescue IL-2 deficient cell memory indicsting paracrine IL-2 is not effective (23,24). Here, we show higher peptide avidity at the effector checkpoint, does not drive greater division of 6d effectors, but does proportionally increase their level of IL-2 production and leads to a dramatic increase in short term effector survival and recovery, such that the number of effectors at 9d (Fig. 3D) is proportional to the size of the memory population at 21d (Fig. 2E). In each organ, there were more than 100-fold higher donor effector cells recovered with the highest peptide vs. no peptide, with very few donor cells in the unpulsed groups (spleen ~10^3, dLN ~500 and lung ~50). At this timepoint even the low avidity peptide results in 20–40-fold more effector cells than no peptide (Fig. 3D). The increase in IL-2 production by effectors at 6d which is determined by peptide avidity and dose of peptide (Fig. 3), clearly links the effect of peptide avidity to IL-2 rescue of effectors and thus increased memory formation. We found IL-2 complexes added at 6–8 dpi, improved the responses to a lower

affinity peptide epitope (Fig 4A–D), producing almost equal number of memory CD4 T cells as the high avidity ones, further supporting that the availability of IL-2 is the key factor that determines the efficiency by which CD4 effector cells transition to memory.

However, our analyses indicate CD25 was either transiently expressed or not expressed on most CD4 effectors, raising the possibility that optimum autocrine IL-2-mediated survival of effectors might be regulated by a mechanism in addition to IL-2 binding to the tripartite IL-2R complex on the CD4 T cell. Another survival cytokine, IL-15, which shares IL-2Rβ/γ with IL-2, is presented *in trans* when bound to IL-15Rα on APC while signaling through IL-2Rβ/γ on the T cell (41–43) and previous studies reported that activated APC can express CD25 in both mice and humans (44, 61). We found the activated BMDC we use as APC and in previous transfer models (Fig 4E), as well as a substantial subset of activated APC in mice infected with influenza 4–8 d earlier (Fig 4F), express high levels of CD25. We tested CD25-deficient APC for their ability to promote memory formation at the checkpoint From CD4 effectors and found they generated fewer memory cells compared to WT APC *in vivo* (Fig. 4). This suggests that Ag/APC transpresent autocrine IL-2 to the interacting CD4 T cells and thus increase IL-2 availability.

We speculate that this autocrine IL-2 transpresentation may play a particularly important role at the checkpoint because most CD4 effectors do not express CD25, and that it helps by driving greater effector survival and better memory formation. We suggest influenza infection also provides pathogen recognition signals that continue to activate APC until virus is cleared, enhancing CD25 expression, as well as MHC-II and costimulatory ligand expression, so that during cognate interaction APC efficiently present both peptide Ag and CD4 effector-produced IL-2. All the results together illustrates the dominant role of IL-2 availability in supporting memory generation from effectors at the checkpoint.

We suggest this set of mechanisms evolved to require that memory develops best only when infection is still ongoing at the effector stage and can therefore provides high avidity peptide Ag at high doses, and high levels of pathogen recognition signals, to promote optimum effector transition to memory, especially in the lung, which is the site of infection. Thus, effective vaccine strategies likely need to provide such high dose, high avidity Ag and pathogen recognition signals during the T cell effector phase, something non-replicating or non pathogen Ag are unlikely to do.

In adult humans, with a long history of exposure to influenza viruses, many responses likely stem from existing memory cells (50–52). We find that efficient generation of 2° memory also requires effector checkpoint Ag recognition and is increased by high avidity interactions (Fig. 6). This contrasts with observations that memory responses in general are less dependent on Ag dose and costimulation (49). We suggest that effector functions of memory cells are more easily achieved, but that forming new secondary memory is again under the stringent regulation to avoid unnecessary memory cells to non-pathogens and select only those with high affinity for persistent Ag only when infection is ongoing.

The impressive impact of Ag avidity for TCR on the size of the memory pool from both primary (Fig. 2) and secondary (Fig. 6) CD4 effectors strongly suggests that both

a high dose of available peptides and CD4 effectors bearing TCR with high affinity for some of those peptides are strictly required for robust memory generation. This implies that immunization with a wide range of viral proteins, including those with known immunodominant CD4 epitopes, will be more effective in inducing memory then single proteins. Because of the heterogeneity of human HLA molecules, only a fraction of total potential viral epitopes will be immunodominant in a given individual, which further argues for vaccines expressing a wide breadth of proteins. A broader repertoire of high affinity memory CD4 T cells should lower the likelihood that escape variants, which arise by random mutations and selection, will have the opportunity to develop and escape so they can be passed on, since this would need require multiple mutations. Many of the immunodominant T cell epitopes, such as the FluNP NP_{311} used here, are in core proteins of viruses, not in the viral surface proteins that B cells recognize, thus it follows that vaccines should include core as well as surface protein epitopes, to elicit both T and B cell immune memory including heterosubtypic determinants not likely to be selected by Ab to external surface proteins.

An advantage of vaccines is that they can supply these signals in a less dangerous context than infection.

Additional studies are needed to support these later implications in detail, but we suggest that the evolutionary advantage of this requirement for a high avidity interaction at the effector stage is to generate memory cells with higher affinity for the infecting virus, while not allowing memory when virus does not persist at high levels into the effector stage, or when there is no replicating infectious entity.

Supplementary Material

Refer to Web version on PubMed Central for supplementary material.

Funding:

This work was supported by National Institutes of Health grants: R01AI118820, R21AI153120, R21AI146532 (to S.L.S), U19 AI109858 (to LJS and ESH) and T32AI007349-30 (MCJ and OKU) and T32 AI132152 (OKU), R21 AI146647 (to KKM) and R21 AI117457 (to TMS).

References

1. McKinstry KK, Strutt TM, Kuang Y, Brown DM, Sell S, Dutton RW, and Swain SL. 2012. Memory CD4+ T cells protect against influenza through multiple synergizing mechanisms. J Clin Invest 122: 2847–2856. [PubMed: 22820287]
2. Obst R, van Santen H-M, Mathis D, and Benoist C. 2005. Antigen persistence is required throughout the expansion phase of a CD4+ T cell response. J Exp Med 201: 1555–1565. [PubMed: 15897273]
3. Prlic M, Hernandez-Hoyos G, and Bevan MJ. 2006. Duration of the initial TCR stimulus controls the magnitude but not functionality of the CD8+ T cell response. J Exp Med 203: 2135–2143. [PubMed: 16908626]
4. Rabenstein H, Behrendt AC, Ellwart JW, Naumann R, Horsch M, Beckers J, and Obst R. 2014. Differential kinetics of antigen dependency of CD4+ and CD8+ T cells. J Immunol 192: 3507–3517. [PubMed: 24639353]

5. Corse E, Gottschalk RA, and Allison JP. 2011. Strength of TCR–Peptide/MHC Interactions and In Vivo T Cell Responses. J Immunol 186: 5039–5045. [PubMed: 21505216]
6. Hosken BNA, Shibuya K, Heath AW, Murphy KM, and Garra AO. 1995. The effect of antigen dose on CD4+ T helper cell phenotype development in a T cell receptor-alpha beta-transgenic model. J Exp Med 182: 1579–1584. [PubMed: 7595228]
7. Brogdon JL, Leitenberg D, and Bottomly K. 2002. The Potency of TCR Signaling Differentially Regulates NFATc/p Activity and Early IL-4 Transcription in Naive CD4+ T Cells. J Immunol 168: 3825–3832. [PubMed: 11937535]
8. Constant BS, Pfeiffer C, Woodard A, Pasqualini T, and Bottomly K. 1995. Extent of T cell receptor ligation can determine the functional differentiation of naive CD4+ T cells. J Exp Med 182: 1591–1596. [PubMed: 7595230]
9. Tubo NJ, Pagán AJ, Taylor JJ, Nelson RW, Linehan JL, Ertelt JM, Huseby ES, Way SS, and Jenkins MK. 2013. Single Naive CD4+ T Cells from a Diverse Repertoire Produce Different Effector Cell Types during Infection. Cell 153: 785–796. [PubMed: 23663778]
10. Fazilleau N, McHeyzer-Williams LJ, Rosen H, and McHeyzer-Williams MG. 2009. The function of follicular helper T cells is regulated by the strength of T cell antigen receptor binding. Nat Immunol 10: 375. [PubMed: 19252493]
11. Keck S, Schmaler M, Ganter S, Wyss L, Oberle S, Huseby ES, Zehn D, and King CG. 2014. Antigen affinity and antigen dose exert distinct influences on CD4 T-cell differentiation. Proc Natl Acad Sci USA 111: 14852–14857. [PubMed: 25267612]
12. Kotov DI, Mitchell JS, Pengo T, Ruedl C, Way SS, Langlois RA, Fife BT, and Jenkins MK. 2019. TCR Affinity Biases Th Cell Differentiation by Regulating CD25, Eef1e1, and Gbp2. J Immunol 202: 2535–2545. [PubMed: 30858199]
13. Snook JP, Kim C, and Williams MA. 2018. TCR signal strength controls the differentiation of CD4+ effector and memory T cells. Sci Immunol 3: 1–13.
14. Busch DH, Pilip I, and Pamer EG. 1998. Evolution of a complex T cell receptor repertoire during primary and recall bacterial infection. J Exp Med 188: 61–70. [PubMed: 9653084]
15. Crawford F, Kozono H, White J, Marrack P, and Kappler J. 1998. Detection of antigen-specific T cells with multivalent soluble class II MHC covalent peptide complexes. Immunity 8: 675–682. [PubMed: 9655481]
16. Busch DH, and Pamer EG. 1999. T cell affinity maturation by selective expansion during infection. J Exp Med 189: 701–709. [PubMed: 9989985]
17. Savage PA, Boniface JJ, and Davis MM. 1999. A kinetic basis for T cell receptor repertoire selection during an immune response. Immunity 10: 485–492. [PubMed: 10229191]
18. Sabatino JJ Jr., Huang J, Zhu C, and Evavold BD. 2011. High prevalence of low affinity peptide-MHC II tetramer-negative effectors during polyclonal CD4+ T cell responses. J Exp Med 208: 81–90. [PubMed: 21220453]
19. Malherbe L, Hausl C, Teyton L, and McHeyzer-Williams MG. 2004. Clonal selection of helper T cells is determined by an affinity threshold with no further skewing of TCR binding properties. Immunity 21: 669–679. [PubMed: 15539153]
20. Corse E, Gottschalk RA, Krogsgaard M, and Allison JP. 2010. Attenuated T cell responses to a high-potency ligand in vivo. PLoS Biol 8.
21. Xia J, Kuang Y, Liang J, Jones M, and Swain SL. 2020. Influenza Vaccine-Induced CD4 Effectors Require Antigen Recognition at an Effector Checkpoint to Generate CD4 Lung Memory and Antibody Production. J Immunol 205: 2077–2090. [PubMed: 32929040]
22. Powell TJ, Strutt T, Reome J, Hollenbaugh JA, Roberts AD, Woodland DL, Swain SL, and Dutton RW. 2007. Priming with cold-adapted influenza A does not prevent infection but elicits long-lived protection against supralethal challenge with heterosubtypic virus. J Immunol 178: 1030–1038. [PubMed: 17202366]
23. Bautista BL, Devarajan P, McKinstry KK, Strutt TM, Vong AM, Jones MC, Kuang Y, Mott D, and Swain SL. 2016. Short-Lived Antigen Recognition but Not Viral Infection at a Defined Checkpoint Programs Effector CD4 T Cells To Become Protective Memory. J Immunol 197: 3936–3949. [PubMed: 27798159]

24. McKinstry KK, Strutt TM, Bautista B, Zhang W, Kuang Y, Cooper AM, and Swain SL. 2014. Effector CD4 T-cell transition to memory requires late cognate interactions that induce autocrine IL-2. Nat Commun 5: 5377. [PubMed: 25369785]
25. Zhang BX, Giangreco L, Broome HE, Dargan CM, and Swain SL. 1995. Control of CD4 effector fate: transforming growth factor beta 1 and interleukin 2 synergize to prevent apoptosis and promote effector expansion. J Exp Med 182: 699–709. [PubMed: 7650478]
26. Moran AE, Holzapfel KL, Xing Y, Cunningham NR, Maltzman JS, Punt J, and Hogquist KA. 2011. T cell receptor signal strength in Treg and iNKT cell development demonstrated by a novel fluorescent reporter mouse. J Exp Med 208: 1279–1289. [PubMed: 21606508]
27. Stadinski BD, Trenh P, Smith RL, Bautista B, Huseby PG, Li G, Stern LJ, and Huseby ES. 2011. A role for differential variable gene pairing in creating T cell receptors specific for unique major histocompatibility ligands. Immunity 35: 694–704. [PubMed: 22101158]
28. Huseby ES, Sather B, Huseby PG, and Goverman J. 2001. Age-dependent T cell tolerance and autoimmunity to myelin basic protein. Immunity 14: 471–481. [PubMed: 11336692]
29. Zhumabekov T, Corbella P, Tolaini M, and Kioussis D. 1995. Improved version of a human CD2 minigene based vector for T cell-specific expression in transgenic mice. Journal of Immunological Methods 185: 133–140. [PubMed: 7665895]
30. Brahmakshatriya V, Kuang Y, Devarajan P, Xia J, Zhang W, Vong AM, and Swain SL. 2017. IL-6 Production by TLR-Activated APC Broadly Enhances Aged Cognate CD4 Helper and B Cell Antibody Responses In Vivo. J Immunol 198: 2819–2833. [PubMed: 28250157]
31. Marshall NB, Vong AM, Devarajan P, Brauner MD, Kuang Y, Nayar R, Schutten EA, Castonguay CH, Berg LJ, Nutt SL, and Swain SL. 2017. NKG2C/E Marks the Unique Cytotoxic CD4 T Cell Subset, ThCTL, Generated by Influenza Infection. J Immunol 198: 1142–1155. [PubMed: 28031335]
32. Devarajan P, Vong AM, Castonguay CH, Kugler-Umana O, Bautista BL, Jones MC, Kelly KA, Xia J, and Swain SL. 2022. Strong influenza-induced TFH generation requires CD4 effectors to recognize antigen locally and receive signals from continuing infection. Proc Natl Acad Sci USA 119.
33. McKinstry KK, Golech S, Lee WH, Huston G, Weng NP, and Swain SL. 2007. Rapid default transition of CD4 T cell effectors to functional memory cells. J Exp Med 204: 2199–2211. [PubMed: 17724126]
34. McKinstry KK, Strutt TM, and Swain SL. 2010. Regulation of CD4+ T-cell contraction during pathogen challenge. Immunological Reviews 236: 110–124. [PubMed: 20636812]
35. Dhume K, Finn CM, Strutt TM, Sell S, and McKinstry KK. 2019. T-bet optimizes CD4 T-cell responses against influenza through CXCR3-dependent lung trafficking but not functional programming. Mucosal Immunol 12: 1220–1230. [PubMed: 31278374]
36. Nanaware PP, Jurewicz MM, Clement CC, Lu L, Santambrogio L, and Stern LJ. 2021. Distinguishing Signal From Noise in Immunopeptidome Studies of Limiting-Abundance Biological Samples: Peptides Presented by I-A(b) in C57BL/6 Mouse Thymus. Front Immunol 12: 658601.
37. Itoh Y, Kajino K, Ogasawara K, Takahashi A, Namba K, Negishi I, Matsuki N, Iwabuchi K, Kakinuma M, Good RA, and Onoé K. 1997. Interaction of pigeon cytochrome c-(43–58) peptide analogs with either T cell antigen receptor or I-Ab molecule. Proc Natl Acad Sci U S A 94: 12047–12052. [PubMed: 9342360]
38. Zhu Y, Rudensky AY, Corper AL, Teyton L, and Wilson IA. 2003. Crystal structure of MHC class II I-Ab in complex with a human CLIP peptide: prediction of an I-Ab peptide-binding motif. J Mol Biol 326: 1157–1174. [PubMed: 12589760]
39. Li J, Huston G, and Swain SL. 2003. IL-7 promotes the transition of CD4 effectors to persistent memory cells. J Exp Med 198: 1807–1815. [PubMed: 14676295]
40. Dhume K, Finn CM, Strutt TM, Sell S, McKinstry KK. T-bet optimizes CD4 T-cell responses against influenza through CXCR3-dependent lung trafficking but not functional programming. Mucosal Immunol. 2019 12:1220–1230. doi: 10.1038/s41385-019-0183-z. [PubMed: 31278374]

41. Lodolce JP, Burkett PR, Boone DL, Chien M, and Ma A. 2001. T cell-independent interleukin 15Rα signals are required for bystander proliferation. J Exp Med 194: 1187–1193. [PubMed: 11602647]
42. Dubois S, Mariner J, Waldmann TA, and Tagaya Y. 2002. IL-15Ra Recycles and Presents IL-15 In trans to Neighboring Cells. Immunity 17: 537–547. [PubMed: 12433361]
43. Stonier SW, and Schluns KS. 2010. Trans-presentation: a novel mechanism regulating IL-15 delivery and responses. Immunol Lett 127: 85–92. [PubMed: 19818367]
44. Wuest SC, Edwan JH, Martin JF, Han S, Perry JS, Cartagena CM, Matsuura E, Maric D, Waldmann TA, and Bielekova B. 2011. A role for interleukin-2 trans-presentation in dendritic cell-mediated T cell activation in humans, as revealed by daclizumab therapy. Nat Med 17: 604–609. [PubMed: 21532597]
45. Eicher DM, and Waldmann TA. 1998. IL-2Rα on one cell can present IL-2 to IL-2Rβ/γc on another cell to augment IL-2 signaling. J Immunol 161: 5430–5437. [PubMed: 9820518]
46. Kim M, Kim TJ, Kim HM, Doh J, and Lee KM. 2017. Multi-cellular natural killer (NK) cell clusters enhance NK cell activation through localizing IL-2 within the cluster. Sci Rep 7: 40623.
47. Swain SL, Jones MC, Devarajan P, Xia J, Dutton RW, Strutt TM, and McKinstry KK. 2021. Durable CD4 T-Cell Memory Generation Depends on Persistence of High Levels of Infection at an Effector Checkpoint that Determines Multiple Fates. Cold Spring Harb Perspect Biol 13.
48. Dubey C, Croft M, and Swain SL. 1995. Costimulatory requirements of naive CD4+ T cells. ICAM-1 or B7–1 can costimulate naive CD4 T cell activation but both are required for optimum response. J Immunol 155: 45–57. [PubMed: 7541426]
49. Strutt TM, McKinstry KK, Kuang Y, Bradley LM, and Swain SL. 2012. Memory CD4+ T-cell-mediated protection depends on secondary effectors that are distinct from and superior to primary effectors. Proc Natl Acad Sci USA 109: E2551–2560. [PubMed: 22927425]
50. Beura LK, Hamilton SE, Bi K, Schenkel JM, Odumade OA, Casey KA, Thompson EA, Fraser KA, Rosato PC, Filali-Mouhim A, Sekaly RP, Jenkins MK, Vezys V, Haining WN, Jameson SC, and Masopust D. 2016. Normalizing the environment recapitulates adult human immune traits in laboratory mice. Nature 532: 512–516. [PubMed: 27096360]
51. Reese TA, Bi K, Kambal A, Filali-Mouhim A, Beura LK, Burger MC, Pulendran B, Sekaly RP, Jameson SC, Masopust D, Haining WN, and Virgin HW. 2016. Sequential Infection with Common Pathogens Promotes Human-like Immune Gene Expression and Altered Vaccine Response. Cell Host Microbe 19: 713–719. [PubMed: 27107939]
52. Herati RS, Muselman A, Vella L, Bengsch B, Parkhouse K, Del Alcazar D, Kotzin J, Doyle SA, Tebas P, Hensley SE, Su LF, Schmader KE, and Wherry EJ. 2017. Successive annual influenza vaccination induces a recurrent oligoclonotypic memory response in circulating T follicular helper cells. Sci Immunol 2.
53. Vanguri V, Govern CC, Smith R, and Huseby ES. 2013. Viral antigen density and confinement time regulate the reactivity pattern of CD4 T-cell responses to vaccinia virus infection. Proc Natl Acad Sci USA 110: 288–293. [PubMed: 23248307]
54. Kim C, Wilson T, Fischer KF, and Williams MA. 2013. Sustained interactions between T cell receptors and antigens promote the differentiation of CD4(+) memory T cells. Immunity 39: 508–520. [PubMed: 24054329]
55. Cho YL, Flossdorf M, Kretschmer L, Hofer T, Busch DH, and Buchholz VR. 2017. TCR Signal Quality Modulates Fate Decisions of Single CD4(+) T Cells in a Probabilistic Manner. Cell Rep 20: 806–818. [PubMed: 28746867]
56. Williams MA, Ravkov EV, and Bevan MJ. 2008. Rapid culling of the CD4+ T cell repertoire in the transition from effector to memory. Immunity 28: 533–545. [PubMed: 18356084]
57. León B, Ballesteros-Tato A, Randall TD, and Lund FE. 2014. Prolonged antigen presentation by immune complex–binding dendritic cells programs the proliferative capacity of memory CD8 T cells. J Exp Med 211: 1637–1655. [PubMed: 25002751]
58. Ballesteros-Tato A, Leon B, Lee BO, Lund FE, and Randall TD. 2014. Epitope-specific regulation of memory programming by differential duration of antigen presentation to influenza-specific CD8(+) T cells. Immunity 41: 127–140. [PubMed: 25035957]

59. Kohlmeier JE, Cookenham T, Miller SC, Roberts AD, Christensen JP, Thomsen AR, and Woodland DL. 2009. CXCR3 directs antigen-specific effector CD4+ T cell migration to the lung during parainfluenza virus infection. J Immunol 183: 4378–4384. [PubMed: 19734208]

60. Groom JR, and Luster AD. 2011. CXCR3 ligands: redundant, collaborative and antagonistic functions. Immunol Cell Biol 89: 207–215. [PubMed: 21221121]

61. Li J, Lu E, Yi T, and Cyster JG. 2016. EBI2 augments Tfh cell fate by promoting interaction with IL-2-quenching dendritic cells. Nature 533: 110–114. [PubMed: 27147029]

62. Zehn D, Lee SY, Bevan MJ. 2009. Complete but curtailed T-cell response to very low-affinity antigen. Nature. 458:211–214. doi: 10.1038/nature0765728. [PubMed: 19182777]

Key Points:

1. Memory generation from CD4 effectors is proportional to their avidity for Ag/APC.
2. TCR avidity regulates autocrine IL-2 and thus regulates their survival and function.
3. Pathogen recognition activates APC to express CD25 and trans-presents IL-2.

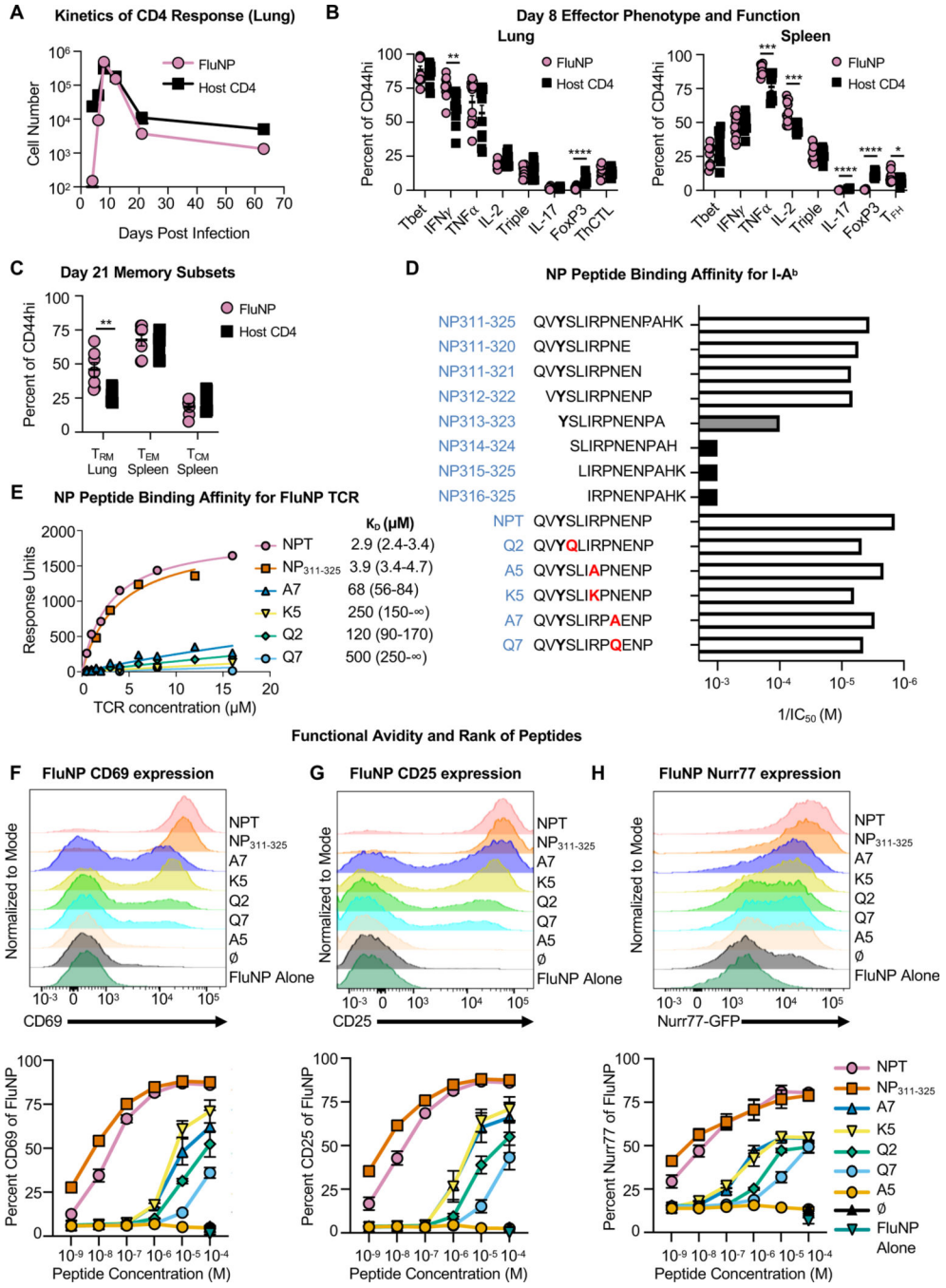

Figure 1: Model to evaluate peptide avidity.

(A-C) Naïve FluNP.Thy1.1$^{+/-}$ cells were transferred to B6 hosts, then infected with PR8. **(A)** Lungs were collected at 4, 6, 8, 12, 21 and 63 dpi and numbers of donor FluNP and responding host CD4^{+}, CD44^{hi} cells were determined by FACS. **(B)** Day 8 Effector phenotype and function. Expression of markers associated with subsets of CD4 effectors were analyzed at 8 dpi in lung and spleen: Th1 (T-Bet^{+}, IL-2^{+}, IFNγ^{+}, TNFα^{+}), Triple positive (IL-2^{+}, IFNγ^{+}, TNFα^{+}), Th17 (IL-17^{+}), Treg (FoxP3^{+}), lung ThCTL (NKG2A/C/E) and spleen T_{FH} (CXCR5^{+}, BCL-6^{+}). **(C)** Memory CD4 subsets were analyzed at 21 dpi:

lung T_{RM} ($CD69^+$), spleen T_{EM} ($CD127^+$ $CD44^+$ $CD62L^-$) and spleen T_{CM} ($CD127^+$ $CD44^+$ $CD62L^+$). **(D-H)** Characterization of NP peptide panel. **(D)** Peptide name, aa sequence (P1=**Y**, mutations in red) and the I-A^b binding affinities of the $NP_{311–325}$ length variants and mutants were experimentally determined to identify the I-A^b binding frame. The reciprocal of the IC_{50} is shown. **(E)** Maximal response for a given TCR concentration was plotted for each peptide-MHC complex and nonlinear fits were generated using the equation $Y=Bmax*X/(K_D + X)$. The fit was constrained to share a consistent Bmax and yield a K_D value of <500. The resulting K_D values are shown in μM with 95% confidence intervals. **(F-H)** Naïve FluNP CD4 T cells were co-cultured with BMDC pulsed with each of the NP peptides for 2d *in vitro*. Induction of markers functionally associated with TCR signal strength was measured. **(F)** CD69; **(G)** CD25; and **(H)** Nur77. Top histograms display level of marker expression following stimulation with Ag/APC pulsed at 10^{-4} M. Bottom displays dose response curve to a broad range of peptide concentrations used to pulse APC. The rank of peptide functional avidity is shown on right. Statistical evaluations: (A) Days 4, 6, 8, 21, 63 Pooled data, n = 9–10, two experiments. Day 12 one experiment n = 5. Mean +/− SEM. (B) Pooled data, n = 11, two experiments, mean +/− SEM. (C) Pooled data, n = 7, two experiments, mean +/− SEM. (D) Pooled data, n=3–4, two experiments. (E-G) Representative data, n = 6, two experiments. (F-H) Pooled data, n = 6, two experiments, mean +/− SEM (% of FluNP). Statistical significance determined by two-tailed independent t test (*p<0.05, **p<0.01, ***p<0.001, ****p<0.0001).

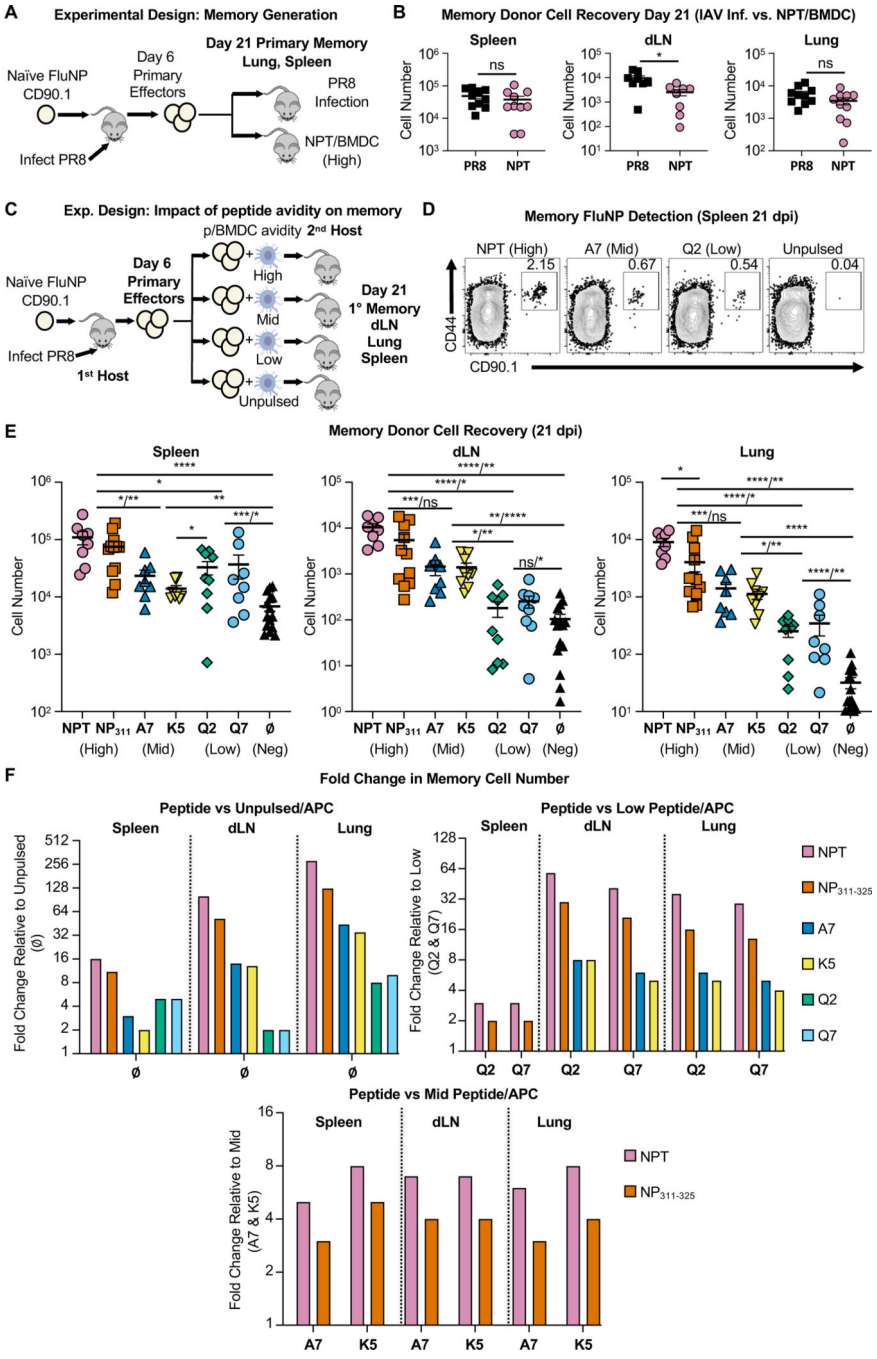

Figure 2: Peptide avidity during the primary effector phase dictates the size of the memory population.

(A) Experimental design: comparison of PR8 infection to high peptide/APC memory generation. Naïve FluNP.Thy1.1$^{+/-}$ cells were transferred to B6 hosts, then infected with PR8. At 6 dpi, FluNP effector cells were isolated from the 1st hosts and co-transferred with either peptide Ag/APC into uninfected 2nd hosts or without APC into day 6 PR8 infection matched hosts (infected 6d previously). Fifteen days later (21 dpi) 2nd hosts were sacrificed, and donor FluNP cells were analyzed by FACS. **(B)** FluNP cell numbers were enumerated

by FACS in the dLN, lung and spleen at 21 dpi. **(C)** Experimental design: Impact of peptide avidity on memory generation. 1.5×10^6 6d FluNP effectors were co-transferred with Ag/APC into uninfected 2nd hosts. The panel of different peptides was used to pulse groups of activated BMDC yielding peptide/APC with different avidity for the TCR of the FluNP T cells. **(D)** Representative FACS plots showing donor FluNP memory cells by CD44 and CD90.1 expression in the spleen at 21 dpi. **(E)** Number of FluNP memory cells detected at 21 dpi in the dLN, lung and spleen of second hosts. Statistical significance determined by two-tailed independent t test (*p<0.05, **p<0.01, ***p<0.001, ****p<0.0001). Spleen comparisons: highs vs. unpulsed, highs vs. lows, NPT vs. A7 / highs vs. K5; mids vs. unpulsed, K5 vs. Q2; Q2 vs. unpulsed / Q7 vs. unpulsed. dLN comparisons: NPT vs. unpulsed / $NP_{311–325}$ vs. unpulsed, NPT vs. lows / $NP_{311–325}$ vs. lows, NPT vs. mids / $NP_{311–325}$ vs. mids; A7 vs. unpulsed / K5 vs. unpulsed, A7 vs. lows / K5 vs. lows; Q2 vs. unpulsed / Q7 vs. unpulsed. Lung comparisons: NPT vs. $NP_{311–325}$; NPT vs. unpulsed / $NP_{311–325}$ vs. unpulsed, NPT vs. lows / $NP_{311–325}$ vs. lows, NPT vs. mids / $NP_{311–325}$ vs. mids; mids vs. unpulsed, mids vs. Q2 / mids vs. Q7; Q2 vs. unpulsed / Q7 vs. unpulsed. **(F)** FluNP cell number fold change relative to unpulsed (left), low peptide-pulsed (right) and mid peptide (below) in dLN, lung and spleen 21 dpi, x-axis lists fold change denominator. (B) Pooled data, n = 10, three experiments, mean +/− SEM. (D) Representative data, n = 8–15, four experiments. (E-F) Pooled data, n = 8–15, four experiments, mean +/− SEM.

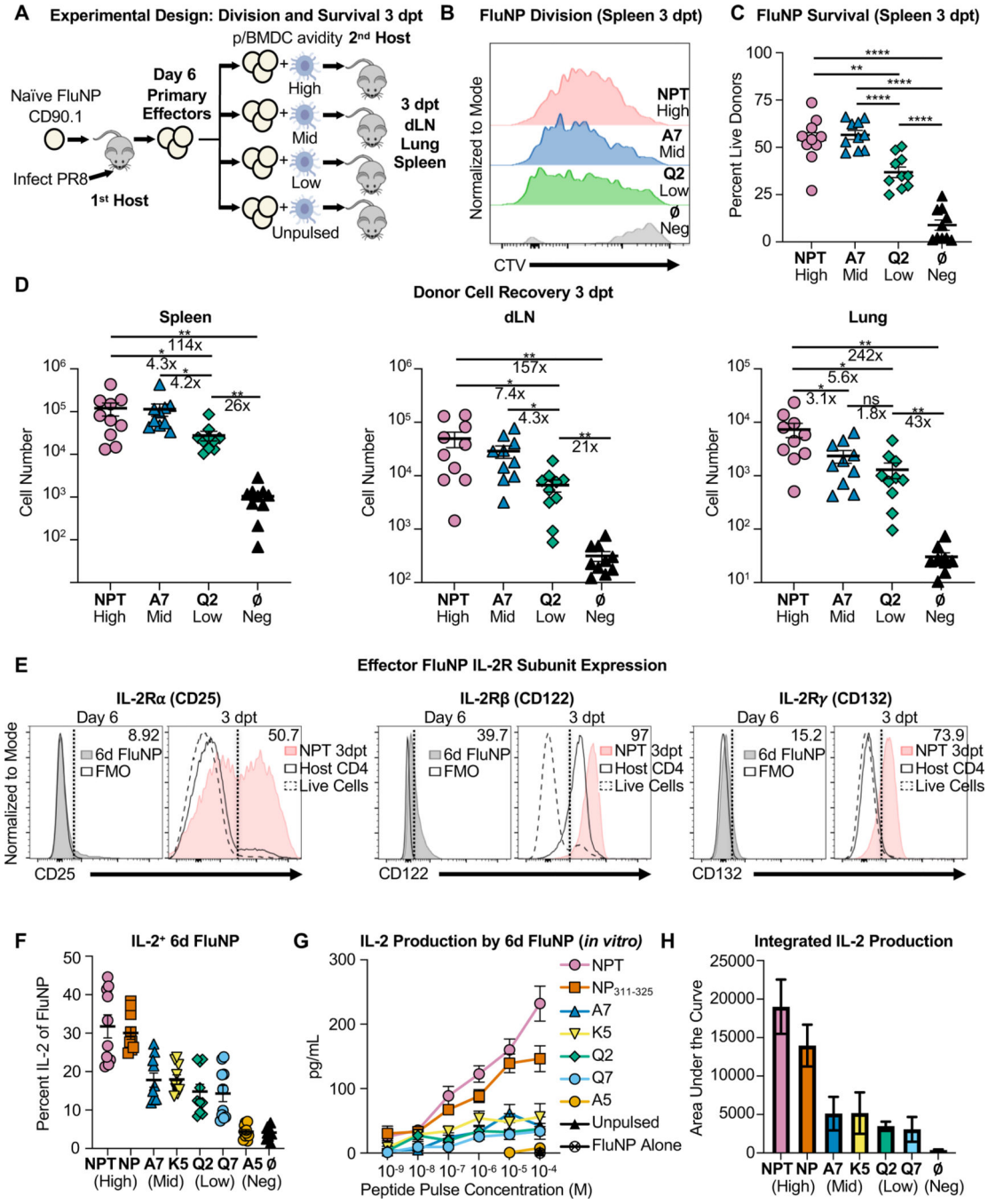

Figure 3: Peptide avidity determines survival but not proliferation of donor cells 3 days post transfer.

(A) Experimental Design. Naïve FluNP CD4 T cells were transferred to B6 hosts, infected with PR8. At 6 dpi, FluNP effector cells were isolated from the 1st host, labeled with cell trace violet (CTV) and transferred to 2nd hosts given 10^6 APC, pulsed or not, with high, mid or low peptides. At 3 days post transfer (dpt), 2nd hosts were sacrificed and FluNP ($CD4^+$ $CD90.1^+$) cells were analyzed. **(B)** Representative FACS plots of FluNP CTV dilution in spleen 3 dpt. Gated on live singlets, $CD4^+$, $CD90.1^+$ cells. **(C)** Percent survival of FluNP

effectors measured by live/dead and caspase 3/7 FACS (double-negative) in spleen 3 dpt. **(D)** Number of donor FluNP cells recovered 3 dpt in the dLN, lung and spleen. **(E)** IL-2 receptor subunit expression: IL-2Rα (CD25), IL-2Rβ (CD122) and IL-2Rγ (CD132) expression was determined by FACS analysis of the 6 dpi effectors (left) and 3 dpt donor cells (right). **(F)** FluNP 6 dpi effectors were restimulated for 6 hours with indicated NP peptides at 10 μM and IL-2 expression determined by FACS. **(G)** FluNP effectors were co-cultured with NP peptide-pulsed APC for 48 hr and IL-2 production in the supernatant was determined by ELISA. **(H)** The area under the curve was calculated to quantitate impact on IL-2 production. (B) Representative data, n = 10, two experiments. (C-E) Pooled data, n = 10, two experiments, mean +/− SEM. (F) Pooled data, n = 10, two experiments, mean +/− SEM. (G-H) Pooled data, n = 3–6, two experiments, mean +/− SEM.

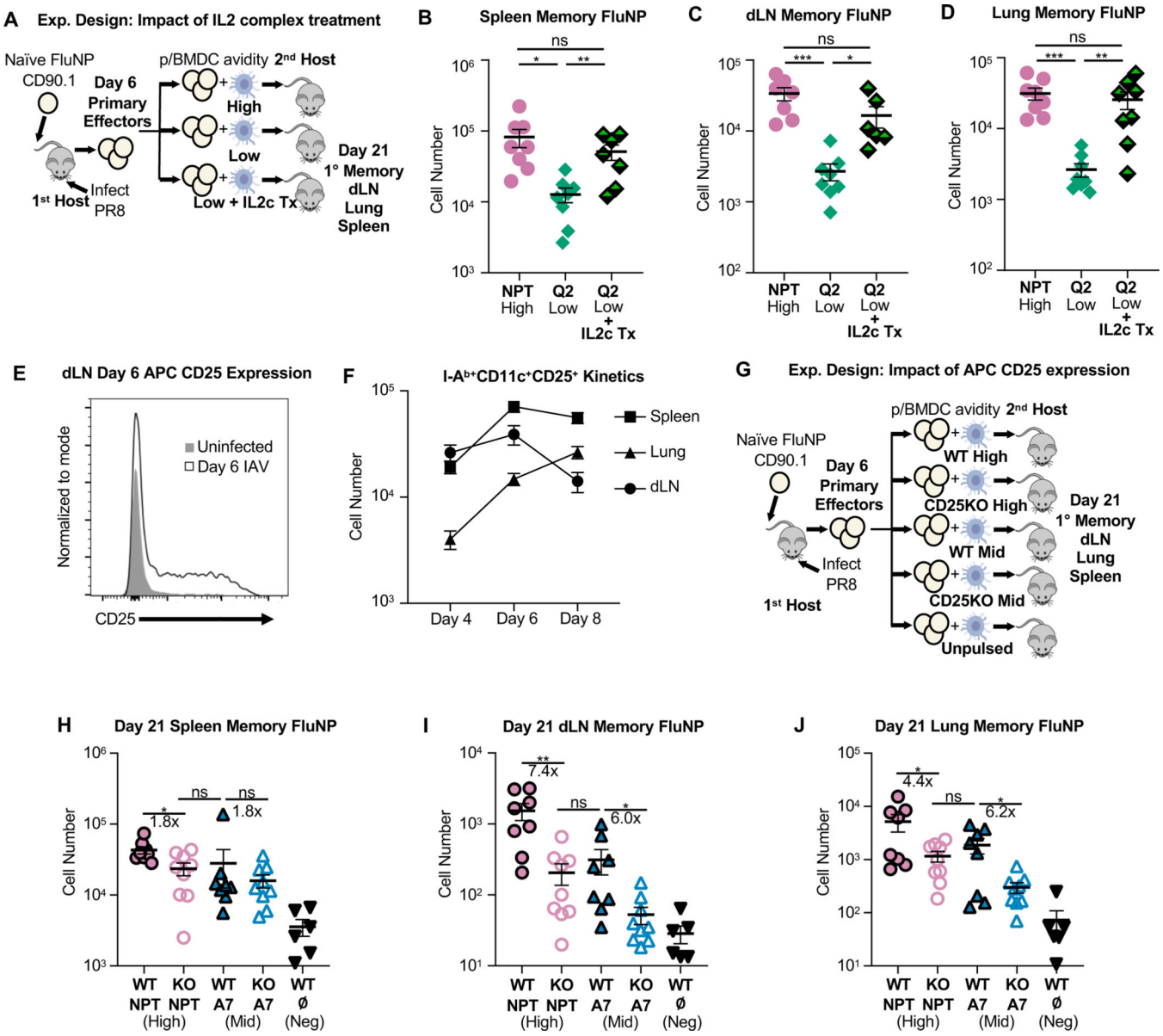

Figure 4: IL-2c Treatment when Ag/APC are low affinity and CD25 Expression on APC Enhance Memory Generation.

(A-D) IL-2 complex treatment (IL-2c tx) rescues low stimulated FluNP memory cells. **(A)** Experimental design. 6 dpi FluNP effectors were co-transferred with NPT (high) or Q2 (low) peptide-pulsed WT BMDC and mice received PBS or IL-2c tx i.p for 3 days post transfer. Number of memory FluNP cells determined by FACS analysis in **(B)** spleen, **(C)** dLN and **(D)** lung. **(E-F)** CD25 Expression on APC *in vivo.* Mice were infected or not with PR8 influenza and sacrificed 4, 6 and 8 dpi. **(E)** CD25 expression was measured by FACS staining on I-A^{b+}, $CD11c^{+}$ cells in the dLN of infected (black line, no fill) or uninfected (gray) mice. **(F)** Kinetics of $CD25^{+}$ I-A^{b+}, $CD11c^{+}$ cells in the dLN, lung, and spleen of infected mice at 4, 6 and 8 dpi. **(G-J)** Impact of CD25 deletion in APC on memory generation. **(G)** Experimental Design. 6 dpi FluNP effectors were co-transferred

with peptide-pulsed WT or CD25KO BMDC to uninfected 2nd hosts. 2nd hosts were sacrificed 15 dpt (21 dpi), and donor memory cells were analyzed by FACS. Number of memory FluNP cells determined by FACS analysis in **(H)** spleen, **(I)** dLN and **(J)** lung. (B-D) Pooled data, n = 7–8, two experiments, mean +/− SEM. (E) Representative data, n = 10, two experiments. (F) Pooled data, n = 9–10, two experiments, mean +/− SEM. (H-J) Pooled data, n = 6–9, two experiments, mean +/− SEM. Statistical significance determined by two-tailed independent t test (*p<0.05, **p<0.01).

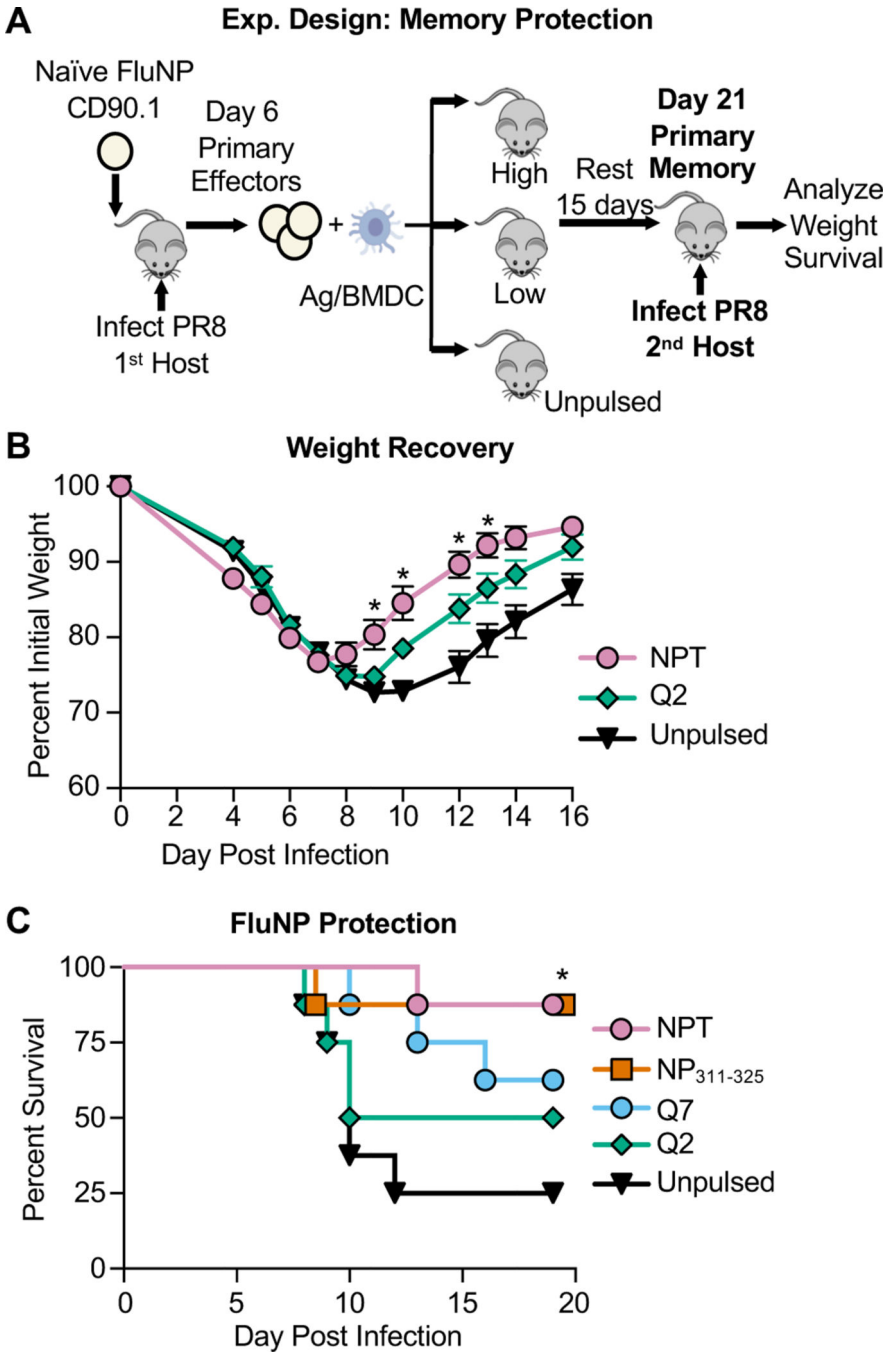

Figure 5: Increased peptide avidity at the effector checkpoint promotes a more protective population of memory cells.

(A) Experimental design: FluNP effector cells (6 dpi) were co-transferred with peptide-pulsed APC into uninfected 2nd hosts and rested for 15 d (21 dpi). At 21 dpi, 2nd hosts were challenged with PR8. **(B)** Weight loss was determined following $2LD_{50}$ PR8 challenge. Statistical significance determined by two-tailed independent t test (*p<0.05). **(C)** Survival was measured following $4LD_{50}$ PR8 challenge. Statistical significance determined by log-rank (Mantel-Cox) test (*p<0.05). (B) Pooled data, n= 10–15, two experiments, mean +/−

SEM. (C) Pooled data, n= 8, two experiments. (E-G) Pooled data, n= 8–9, two experiments, mean +/− SEM.

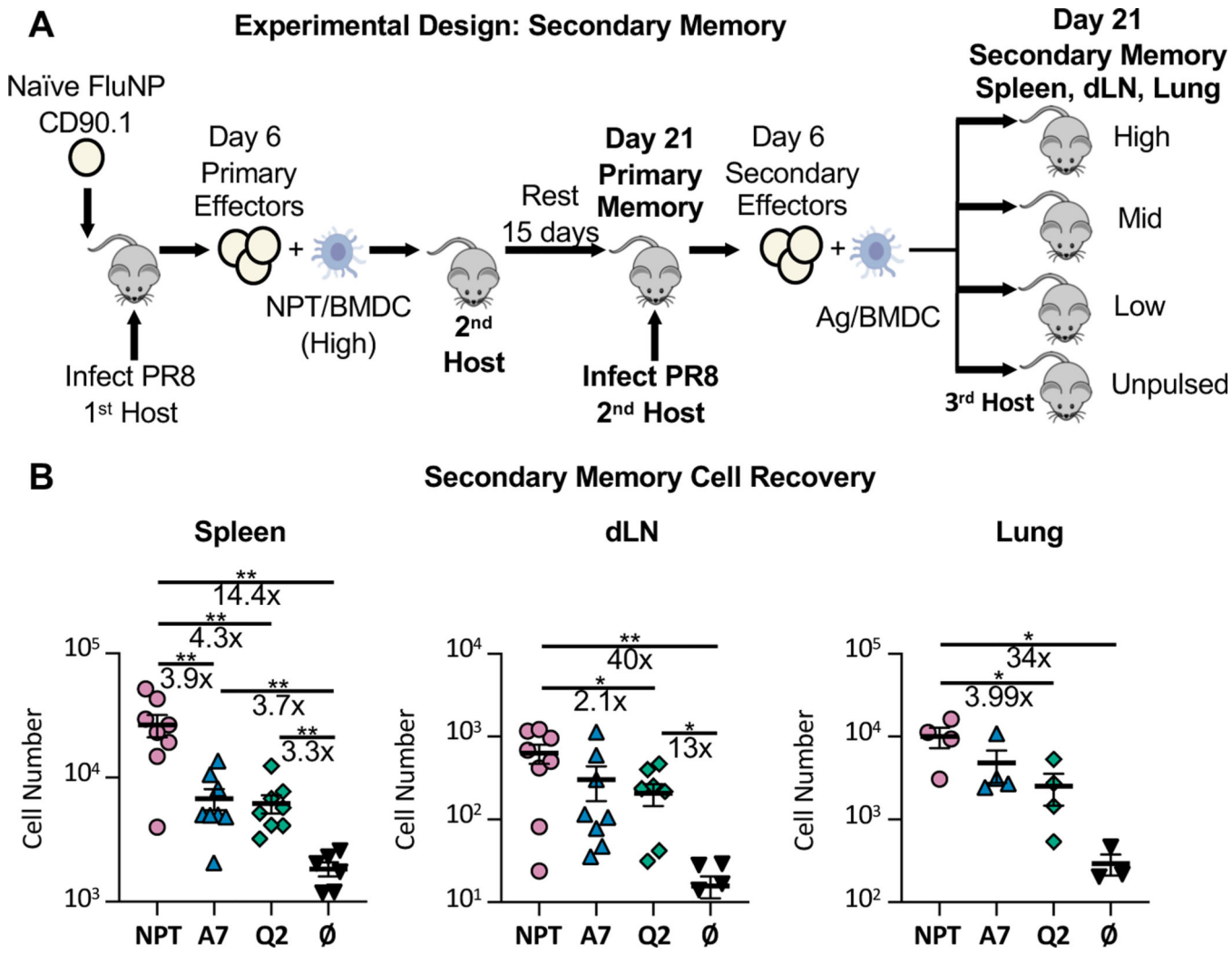

Figure 6: Peptide avidity during the secondary effector checkpoint regulates the size of the secondary memory population.

(A) Experimental design. Primary 6 dpi FluNP effectors were generated and 1.5×10^6 co-transferred to 2nd hosts with 10^6 NPT (high) peptide-pulsed BMDCs. At the memory stage, 21 dpi for the donor cells, 2nd hosts were infected with PR8 influenza (0.3 LD_{50}) and secondary 6 dpi effectors were isolated via CD90.1 MACS and co-transferred to uninfected 3rd hosts. Fifteen days later 3rd hosts were sacrificed, and donor secondary memory cells were analyzed by FACS. **(B)** Number of secondary memory donor FluNP cells determined FACS analysis in the spleen, dLN and lung. Spleen and dLN pooled data, n = 6–8, two experiments, mean +/− SEM. Lung representative data n = 6–8, two experiments, mean +/− SEM. Statistical significance determined by two-tailed independent t test (*p<0.05, **p<0.01).